

Analysis of the Rydberg structure in the vapor-phase electronic absorption spectrum of $(\eta^7\text{-cycloheptatrienyl})(\eta^5\text{-cyclopentadienyl})\text{chromium}$

S. Yu. Ketkov

G. A. Razuvaev Institute of Organometallic Chemistry, Russian Academy of Sciences,
49 ul. Tropinina, 603600 Nizhnii Novgorod, Russian Federation.

Fax: +7 (831 2) 66 1497. E-mail: sketkov@imoc.sinn.ru

Parameters of the Rydberg transitions in the vapor-phase absorption spectrum of $(\eta^7\text{-C}_7\text{H}_7)(\eta^5\text{-C}_5\text{H}_5)\text{Cr}$ were analyzed in detail. A correspondence between the three Rydberg series in the short-wavelength region of the spectrum and low-frequency Rydberg bands was established. Vibronic structure of the observed transitions to the lowest Rydberg s , $p_{x,y}$, p_z , and $d_{xz,yz}$ levels was interpreted. The long-wavelength and short-wavelength series, respectively characterized by quantum defect (δ) values of 1.26 and 0.82, were unambiguously assigned to the Rydberg $p_{x,y}$ and $d_{xz,yz}$ excitations, respectively. Transitions from the $3d_{z^2}$ orbital to the $R(n-1)f$, Rnd_{z^2} , and Rnp_z levels can contribute to the series characterized by a δ value of 1.04. The assignment was made of Rydberg bands in the spectral region corresponding to the principal quantum number (n) values of 5, 6, and 7 (in this region, interpretation of the spectral pattern is complicated because of the band shifts and broadening). At $n > 5$, changes in the δ values of the Rydberg excitations with increase in the n value are due to configuration interaction. The electronic-excited states, which can be responsible for the observed changes in the Rydberg parameters, were determined.

Key words: $(\eta^7\text{-cycloheptatrienyl})(\eta^5\text{-cyclopentadienyl})\text{chromium}$, electronic absorption spectrum, band assignment, Rydberg transitions, vibronic structure, configuration interaction.

Transition-metal sandwich complexes are unique objects for studies by electronic absorption spectroscopy, since currently it is the only class of organometallic compounds whose vapor-phase electronic absorption spectra (EAS) reveal clearly defined Rydberg bands.^{1–22} These bands are due to electron transitions from the nonbonding d_{z^2} orbital of the metal atom to the Rydberg levels. In some instances,^{1–17} it is possible to reveal the spectral series, which are described by the Rydberg formula

$$\nu_n = I - R/(n - \delta) = I - T,$$

where ν_n is the frequency of a series member; I is the ionization limit (IL), which is equal to the energy of detachment of an electron from the d_{z^2} orbital; R is the Rydberg constant; n is the principal quantum number; δ is the quantum defect; and T is the term value, which is the energy of interaction of the Rydberg electron with the cationic core. No Rydberg bands are observed in the EAS on going from the vapor phase to the condensed phase.^{1–22}

Knowing the convergence limit of the Rydberg series, it is possible to determine with high accuracy the ionization potentials (IP) of sandwich complexes.^{1–15} Parameters of Rydberg transitions contain valuable information on the molecular and electronic structure of compounds. Recently, interest in studies of EAS of mixed sandwich

complexes in the vapor phase has grown.^{14–20} Among these compounds, of particular interest is $(\eta^7\text{-cycloheptatrienyl})(\eta^5\text{-cyclopentadienyl})\text{chromium}$ (**1**), whose spectrum reveals the most clearly defined Rydberg structure.¹⁴ The clearly seen short-wavelength Rydberg bands in the vapor-phase EAS of complex **1** made it possible to use it as a reference when analyzing the Rydberg structure in the EAS of mixed sandwich derivatives of molybdenum and tungsten.^{15,16} At the same time, the spectrum of complex **1** was the objective of the preliminary communication¹⁴ only, in which it was shown that the Rydberg structure is described in the framework of the $C_{\infty v}$ point group and several most intense bands were assigned. The unique structurization of the vapor-phase EAS of complex **1** and the possibility of its use for interpreting the spectra of mixed complexes with substituted rings¹⁶ determine the necessity of a detailed analysis of this spectrum, which is the aim of this work.

Experimental

Complex **1** was synthesized according to the known procedure²³ and purified by recrystallization from *n*-heptane followed by vacuum sublimation. Its electronic absorption spectrum was recorded on a Specord UV-VIS spectrometer (Carl Zeiss, Jena) using a heated evacuated quartz cell at 100–140 °C. The spectrometer was calibrated using the UV absorption spectrum of PhH vapors. The spectral resolution was 30 cm^{–1}.

The ionization limits and quantum defects of Rydberg series were calculated on a personal computer using an original program, which makes it possible to minimize the absolute deviations of calculated Rydberg frequencies from experimental ones. The short-wavelength spectral region was analyzed by deconvoluting the contour of the spectral line into Gaussian components.

Results and Discussion

At least three Rydberg series converging on the same IL can be distinguished in the short-wavelength region of the spectrum of complex **1** (Fig. 1). The frequencies of higher members of the series are well described by the Rydberg formula. The experimental and calculated band positions and the parameters of the series are listed in Table 1.

Using the Rydberg series, it is possible to determine with high accuracy the IP of complex **1**.¹⁴ The IL of the series are 45210, 45180, and 45170 cm^{-1} (see Table 1). The first IP of compound **1** can be taken equal to the arithmetic mean of these values, 45190 cm^{-1} (5.603 eV). The error of IL determination is $\pm 40 \text{ cm}^{-1}$ ($\pm 0.005 \text{ eV}$). The value obtained is in good agreement with the position of the first peak in the photoelectron spectrum of complex **1** (5.59,²⁴ 5.61 eV²⁵). Since this peak is due to detachment of an electron from the $3d_{z^2}$ level,^{24,25} all three Rydberg series in the absorption spectrum of

Table 1. Frequencies of higher terms of Rydberg series in the vapor-phase EAS of complex **1**: experimental ($\nu_{\text{exp}}/\text{cm}^{-1}$) and calculated by the Rydberg formula ($\nu_{\text{theor}}/\text{cm}^{-1}$)

<i>n</i>	Series 1 ^a		Series 2 ^b		Series 3 ^c	
	ν_{theor}	ν_{exp}	ν_{theor}	ν_{exp}	ν_{theor}	ν_{exp}
7	41880	41900	42090	42080	42300	42300
8	42790	42760	42910	42900	43040	43050
9	43380	43370	43450	43460	43530	43540
10	43770	43770	43180	—	43870	43870
11	44050	44050	44070	44050	44110	44120
12	44260	44270	44260	44270	44290	22270

^a $I = 45210 \text{ cm}^{-1}$, $\delta = 1.26$.

^b $I = 45180 \text{ cm}^{-1}$, $\delta = 1.04$.

^c $I = 45170 \text{ cm}^{-1}$, $\delta = 0.82$.

complex **1** correspond to transitions from the nonbonding $3d_{z^2}$ MO.

The quantum defect value for the most intense series ($\delta = 1.26$) makes it possible to assign this series to transitions to Rnp levels. However, it is impossible to unambiguously determine the polarization of the transitions using the δ value only, since the quantum defect of the series in question has an intermediate value between those of $Rnp_{x,y}$ and Rnp_z series in the spectrum of isoelectronic $(\eta^6\text{-PhH})_2\text{Cr}$.^{4,7,8,11} Even more ambiguous interpretation based on the values of quantum defects can be made for the other two Rydberg series in the EAS of complex **1**.

More concrete information on the nature of high-frequency Rydberg transitions can be obtained from analysis of the long-wavelength Rydberg bands (Fig. 2) corresponding to each of the three series. In turn, the low-lying Rydberg transitions are interpreted on the basis of analyzing the term values. The term values of the long-wavelength Rydberg 0_0^0 bands in the spectrum of compound **1**, calculated using the IL of the series found in this work, the frequencies of the bands, and the effective principal quantum numbers ($n^* = n - \delta$) are listed in Table 2.

The longest-wavelength band in the vapor-phase EAS of complex **1** ($\nu = 23800 \text{ cm}^{-1}$) is characterized by a T value that coincides with the value of the $R4s$ term for the $(\eta^6\text{-PhH})(\eta^5\text{-Cp})\text{Mn}$ molecule.^{17,18} This makes it possible to interpret this band as the band corresponding to the $3d_{z^2} \rightarrow R4s$ transition. Only the peak at 35500 cm^{-1} (Fig. 3), for which the n^* value increases by 1.10 (see Table 2), can be assigned to the second member of the Rns series.

The strongest long-wavelength peak has a maximum at 27610 cm^{-1} . Based on the corresponding term value (see Table 2), this band can be unambiguously assigned to the 0_0^0 transition to the $R4p_{x,y}$ level. The second member of the $Rnp_{x,y}$ series corresponds to the peak at 35680 cm^{-1} (see Fig. 3), for which the n^* value increases by 1.07 as compared to that of the first member (see Table 2). The term values for these transitions

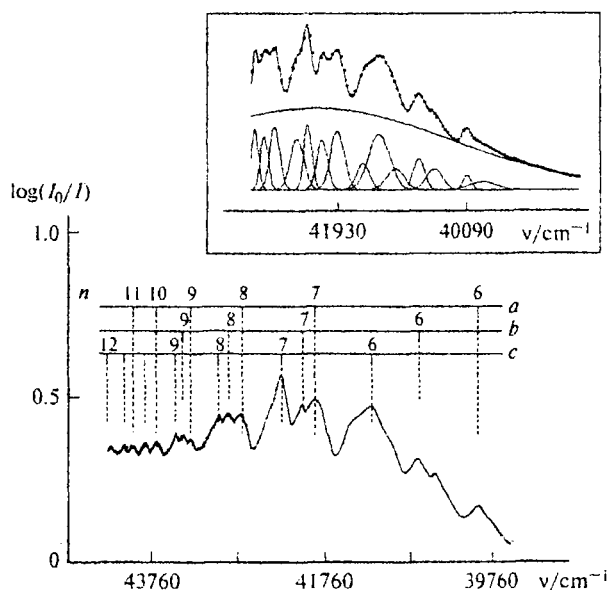


Fig. 1. Short-wavelength Rydberg bands in the vapor-phase EAS of complex **1**: a, series 1, $\delta = 1.26$, $np_{x,y}$; b, series 2, $\delta = 1.04$, $(n-1)f$, nd_{z^2} , np_z ; c, series 3, $\delta = 0.82$, $nd_{xz,yz}$ (here and in Fig. 3, I_0 and I respectively mean the intensity of incident radiation and that of radiation transmitted through the cell filled with the substance). Deconvolution of the spectral region from 39000 to 43000 cm^{-1} into Gaussian components is shown in the inset (the points correspond to the experimental spectrum).

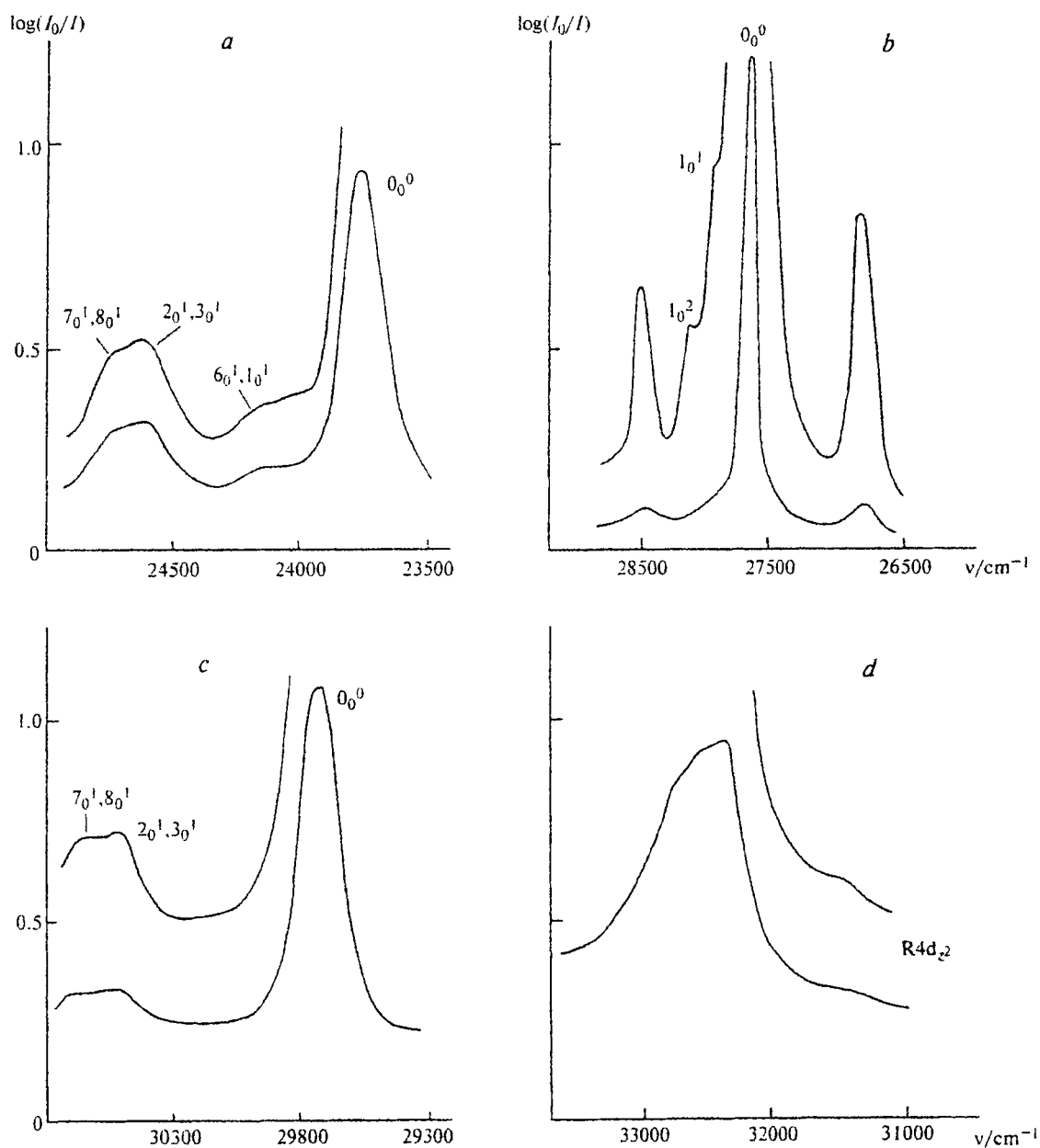


Fig. 2. Long-wavelength Rydberg bands in the vapor-phase EAS of complex 1: *a*, $R4s$; *b*, $R4p_{x,y}$; *c*, $R4p_z$; and *d*, $R4d_{x^2-y^2, xy}$. Vibronic components are denoted as $k_v\nu'$, where k is the number of the normal vibration and ν' and ν are the vibrational quantum numbers in the ground and excited electronic states, respectively.

Table 2. Frequencies (ν/cm^{-1}), term values (T/cm^{-1}), effective principal quantum numbers (n^*), and assignment of low-lying Rydberg bands ($n = 4, 5$) in the EAS of complex 1

$n = 4$				$n = 5$			
ν	T	n^*	Assignment	ν	T	n^*	Assignment
23800	21390	2.27	$R4s$	35500	9690	3.37	$R5s$
27610	17580	2.50	$R4p_{x,y}$	36560	8630	3.57	$R5p_{x,y}$
29700	15490	2.66	$R4p_z$	37430	7760	3.76	$R5p_z$
31560	13630	2.84	$R4d_{z^2}$	37960	7230	3.90	$R4f, R5d_{z^2}$
32440	12750	2.93	$R4d_{x^2-y^2, xy}$				

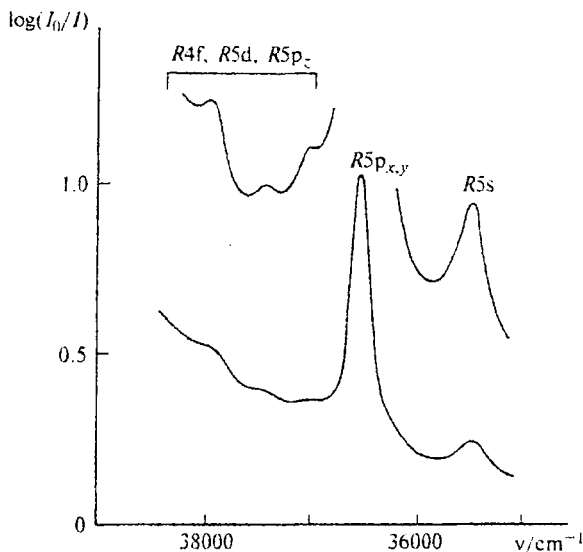


Fig. 3. Rydberg structure of the vapor-phase EAS of complex 1 in the region corresponding to $n = 5$.

in molecule **1** are 200–300 cm^{-1} higher than in $(\eta^6\text{-PhH})_2\text{Cr}$.¹¹

On the basis of the T value the band at 29700 cm^{-1} should be assigned to the 0_0^0 excitation for the $3d_{z^2} \rightarrow R4p_z$ transition. Judging from the T value (see Table 2) for the relatively broad peak with a maximum at 32440 cm^{-1} (see Fig. 2), it can be assigned to one of the $R4d$ excitations. The $3d_{z^2} \rightarrow R4d_{z^2}$ and $3d_{z^2} \rightarrow R4d_{xz,yz}$ transitions are allowed for the $C_{\infty v}$ point group. By analogy with the $R4p$ excitations one should expect that the transition to the degenerate $R4d_{xz,yz}$ level will have a higher intensity. Since there are no other intense bands in the region of $R4d$ transitions in the spectrum of complex **1**, except for the peak at 32440 cm^{-1} , it can be assigned to the $3d_{z^2} \rightarrow R4d_{xz,yz}$ transition. Such an assignment is confirmed by splitting of the corresponding band in the spectrum of $(\eta^7\text{-C}_7\text{H}_7)(\eta^5\text{-C}_5\text{H}_4\text{Me})\text{Mo}$.¹⁶ Then the weak shoulder at 31560 cm^{-1} can be assigned to the transition to the $R4d_{z^2}$ level.

The lowest Rydberg s and p transitions in the spectrum of complex **1** display a vibronic structure (see Fig. 2). As in the case of $(\eta^6\text{-PhH})_2\text{Cr}$,¹¹ a short progression (with an interval of $\sim 200 \text{ cm}^{-1}$) in the totally symmetric metal–ring vibration ν_1 and a peak separated by 830 cm^{-1} from the 0_0^0 transition and corresponding to excitation of the C–H umbrella vibrations ν_3 and ν_4 in the two ligands can be distinguished for the $R4p_{x,y}$ band (since the normal coordinate analysis of the mixed sandwich molecules has not been carried out and there is no generally used notation of vibrational modes in such complexes, we enumerate here only those modes which are observed in the vibronic structure of Rydberg bands). The ν_3 and ν_4 frequencies in the ground electronic state of molecule **1** are equal to 808 cm^{-1} ,²⁶ which is in agreement with this assignment.

A peak at 26720 cm^{-1} separated by 890 cm^{-1} from the 0_0^0 transition is observed on the long-wavelength wing of the $R4p_{x,y}$ band. It is impossible to consider this peak as a "hot" band because of its high relative intensity. Hence, it must be a vibronic component of the lower-lying $R4s$ excitation. In fact, the spacing between this peak and the 0_0^0 transition corresponding to the $3d_{z^2} \rightarrow R4s$ excitation (2920 cm^{-1}) virtually coincides with the frequencies of the C–H π vibrations ν_4 and ν_5 found from the IR spectrum of complex **1** (2933 cm^{-1}).²⁶ An analogous vibronic component was found in the structure of the $R4p_{x,y}$ transition for $(\eta^6\text{-PhH})_2\text{Cr}$.¹¹

Deconvolution of the contour of the spectral line in the region of the $R4s$ band into Gaussian components makes it possible to distinguish the components responsible for excitation of the ν_1 , ν_2 , and ν_3 modes, as well as the peaks separated by 390 and 980 cm^{-1} from the 0_0^0 transition. The first of them can be assigned to the ν_6 mode corresponding to the antisymmetric stretching vibration metal–ring in the $(\eta^6\text{-PhH})_2\text{Cr}$ molecule²⁷ (490 cm^{-1}). In the $C_{\infty v}$ point group, this vibration becomes totally symmetric. The 980 cm^{-1} separation corresponds to the C–H vibrations ν_7 and ν_8 . These modes are responsible for the bands in the region 1000 cm^{-1} in the IR spectrum of complex **1**.²⁶ The components due to ν_7 and ν_8 excitations are also observed in the structure of the $R4p_z$ band (see Fig. 2). The $R4d_{xz,yz}$ transition has no clearly defined elements of vibronic structure, which is either due to the configuration interaction (CI) or to superposition of vibronic components of the $R4d_{z^2}$ and $R4d_{xz,yz}$ excitations. The structure of corresponding band becomes more clearly seen as the Cr atom is replaced by Mo or W atoms.^{15,16}

Interpretation of the Rydberg $R5p_z$ and $R5d$ bands (see Fig. 3) is complicated because of their low relative intensities and possible shifts and broadening of the Rydberg transitions as a result of mixing with valence-shell excitations with close-lying energies. Assuming that the quantum defects for the Rnp and Rnd transitions change much the same as n increases from 4 to 5, it is possible to estimate the expected frequencies for the $R5p_z$, $R5d_{z^2}$, and $R5d_{xz,yz}$ excitations. The values obtained are listed in Table 3.

Three weak bands at 37000, 37430, and 37960 cm^{-1} are observed on the short-wavelength side of the $R5p_{x,y}$ peak (see Fig. 3). Comparison with the expected values (see Table 3) makes it possible to respectively assign the last two bands to transitions to the $R5p_z$ and $5d_{z^2}$ levels. In this case, the shoulder at 37000 cm^{-1} should be interpreted as a vibronic component of the $R5p_{x,y}$ transition. No clearly defined absorption bands are observed in the region 38300 cm^{-1} , where the appearance of the $R5d_{xz,yz}$ peak is expected. This can be explained by broadening of the $R5d_{xz,yz}$ transition caused by CI.

The assignment of transitions corresponding to $n = 6$ and 7 is complicated by the shifts and broadening of Rydberg bands. This can be demonstrated taking the attempt to find a band corresponding to the $3d_{z^2} \rightarrow R6s$

Table 3. Expected frequencies (ν_n/cm^{-1}) of Rydberg transitions in the EAS of complex **1** in the region $n = 5-7$ calculated from the parameters of the lowest Rydberg transitions (A) and higher terms of Rydberg series (B)

Calculation procedure	Transition, series	δ	ν_5	ν_6	ν_7
A	s	1.63	35500*	39440	41380
	$p_{x,y}$	1.43	36560*	39940	41650
	p_z	1.27	37300	40290	41850
	d_{z^2}	1.09	38010	40640	42050
	$d_{xz,yz}$	1.00	38330	40800	42140
B	Series 1	1.26	37340	40310	41860
	Series 2	1.04	38190	40730	42100
	Series 3	0.82	38910	41100	42320
	Series 4	1.64	35470	39420	41370

* Experimental frequencies of $R5s$ and $R5p_{x,y}$ transitions.

transition as an example. At $n = 6$, the frequency calculated by the Rydberg formula using the quantum defect for the $R5s$ excitation is 39440 cm^{-1} . However, no clearly defined bands are observed in this region of the EAS of complex **1** (see Fig. 1), which can be due both to low relative intensity of the $3d_{z^2} \rightarrow R6s$ transition and to its broadening caused by CI. To reveal the broadened Rydberg bands corresponding to $n = 6$ and 7, the region from 39000 to 43000 cm^{-1} in the spectrum of compound **1** was deconvoluted into Gaussian components (see Fig. 1) whose parameters are listed in Table 4.

To interpret the Rydberg structure in the spectral region under study, it is required to establish the correspondence between these Gaussian peaks, the Rydberg series observed, and the lowest Rydberg transitions. To this end, assuming that the values of quantum defects remain constant as n decreases from 7 to 5, we calcu-

Table 4. Positions of maxima (ν/cm^{-1}), halfwidths ($\Delta_{1/2}/\text{cm}^{-1}$), term values (T/cm^{-1}), relative integrated intensities (A_{rel}), effective principal quantum numbers (n^*), and assignment of Gaussian peaks corresponding to the Rydberg bands in the region from 39000 to 43000 cm^{-1} in the EAS of complex **1**

ν	$\Delta_{1/2}$	T	A_{rel}	n^*	Assignment
39780	480	5410	19.3	4.50	$R6s$
40020	150	5170	11.1	4.61	$R6p_{x,y}$
40490	290	4700	32.6	4.83	$R6p_z$
40720	190	4470	30.9	4.95	$R5f, R6d_{z^2}$
41080	300	4110	33.2	5.17	$R5f, R6d_{z^2}$
41300	360	3890	100.0	5.31	$R6d_{xz,yz}$
41540	220	3650	28.5	5.48	$R7s$
41900	220	3290	65.5	5.78	$R7p_{x,y}$
42120	180	3070	43.0	5.98	$R6f, R7p_z, R7d_{z^2}$
42320	130	2870	43.9	6.18	$R7d_{xz,yz}$
42470	230	2720	57.6	6.35	$R8s$
42790	170	2400	53.6	6.76	$R8p_{x,y}$
42940	130	2250	35.8	6.98	$R7f, R8p_z, R8d_{z^2}$
43070	110	2120	32.6	7.19	$R8d_{xz,yz}$

lated expected frequencies of the series members for $n = 5, 6$, and 7. We also calculated expected frequencies of allowed s, p, and d transitions for $n = 6$ and 7 assuming that the δ values remain constant as n increases from 5 to 7. The calculated frequencies are listed in Table 3.

The Gaussian component with a maximum at 39780 cm^{-1} should be assigned to the transition to the $R6s$ level. Its blue shift (340 cm^{-1} from the calculated value) and large width (see Table 4) are indicative of the interaction with a lower-lying excited state. The position of the maximum of the next component (40020 cm^{-1}) is very close to that calculated for the $R6p_{x,y}$ transition (see Table 3). The small band halfwidth (see Table 4) makes it possible to unambiguously assign it to the unperturbed $3d_{z^2} \rightarrow R6p_{x,y}$ excitation. According to calculations (see Table 3), the next member of the $Rnp_{x,y}$ series must lie between the spectral components with maxima at 41540 and 41900 cm^{-1} , the latter belonging to series 1.

As was mentioned above, series 1 is due to transitions to Rnp levels. For this series, the δ value is intermediate between those of the $Rnp_{x,y}$ and Rnp_z series for $(\eta^6\text{-PhH})_2\text{Cr}$.^{7,8,11} The difference between the quantum defects of these series for compounds with closely related molecular and electronic structure indicates that the Rydberg transitions are shifted due to interaction between electronic-excited states.²⁸

Retention of a constant value of the quantum defect for the whole Rydberg series at n greater than a specified value means that the differences between the term values for perturbed and unperturbed Rydberg levels and, hence, the CI energy decreases as the principal quantum number increases. This is possible only if the energy of the perturbing electronic-excited state is lower than that of the series member corresponding to the longest wavelength, for which the δ value remains constant. Then, the energy difference between the Rydberg states and the perturbing state increases as n increases, which leads to decrease in the perturbation energy. The reverse situation should be observed for the Rydberg states interacting with a higher-lying excited state: it is impossible to retain the constant value of the quantum defect in this case.

Thus, it becomes apparent that the members of series 1 in the spectrum of molecule **1** are perturbed by a lower-lying excited level. Such an interaction leads to their blue shift relative to the positions of the unperturbed levels, which means that the δ value decreases on going from $(\eta^6\text{-PhH})_2\text{Cr}$ to complex **1**. Therefore, series 1 in the EAS of compound **1** should be unambiguously assigned to $3d_{z^2} \rightarrow Rnp_{x,y}$ excitations. Interaction between the members of the $Rnp_{x,y}$ series (at $n > 6$) and another symmetry-allowed electronic transition is confirmed by increasing the relative intensity and halfwidth of the peak at 41900 cm^{-1} compared to those of the peak at 40020 cm^{-1} (see Table 4). As in the case of $(\eta^6\text{-PhH})_2\text{M}$ ($\text{M} = \text{Cr, Mo, W}$) complexes,^{4,7-11,13} the

intensities of unperturbed Rydberg excitations decrease as n increases.²⁸ Since the $R6p_{x,y}$ transition reveals no indications of CI, one can conclude that the energy of an excited state admixed to higher-lying $Rnp_{x,y}$ levels is close to that of the $R7p_{x,y}$ state.

A relatively broad Gaussian spectral component at 40490 cm^{-1} (see Table 4) should be assigned to the $R6p_{x,y}$ transition. Its broadening and blue shift by 200 cm^{-1} from the calculated position (see Table 3) can be explained by admixture of a lower-lying excited state, which perturbs the $R6s$ level of the same symmetry.

The position of the peak at 40020 cm^{-1} coincides with that calculated for the member of series 2, corresponding to $n = 6$ (see Table 3). Its small width, comparable with that of the $R6p_{x,y}$ band (see Table 4), indicates that there is no admixture of valence-shell transitions or it is small. This peak can be reliably assigned to series 2. From the data in Table 3 it can be seen that close-lying frequencies are expected for unperturbed $R6d$ transitions. In addition, $R5f$ excitations also fall into the same spectral region, for which one should expect $\delta \approx 0$.²⁸

Since the peak with a maximum at 41300 cm^{-1} (the most intense peak in the spectral region considered) lies between the members of series 2 ($n = 6$) and series 1 ($n = 7$), it must belong to series 3. The calculated frequency of a member of series 3 corresponding to $n = 6$ is 200 cm^{-1} lower than the experimental value (see Table 3), which indicates that the Rydberg level is shifted due to interaction with a lower-lying electronic-excited state. The fact that CI occurs is also confirmed by the relatively large halfwidth of the peak in question (see Table 4). Among lower-lying unperturbed Rydberg transitions, the $3d_{z^2} \rightarrow R6d_{xz,yz}$ transition is the closest to the peak at 41300 cm^{-1} . It is this excitation that is the most probable candidate for assigning the strongest Gaussian component. Assigning series 3 to $Rnd_{xz,yz}$ transitions leads to a logical explanation of changes in the δ value that occur as n increases, which, in turn, is in good agreement with the pattern observed for series 1.

In fact, admixture of an excited state perturbing the $R6d_{xz,yz}$ level to higher $Rnd_{xz,yz}$ states must result in a decrease in the quantum defect as compared with the δ values for unperturbed $Rnd_{xz,yz}$ transitions (see Table 3), which is observed experimentally. The abnormally small δ value for the peak at 41300 cm^{-1} (0.69) indicates that the energy of the perturbing state is very close to that of the $R6d_{xz,yz}$ level. In the case of molecule **1** this is confirmed by the presence of a band with a maximum at 41200 cm^{-1} in the solution-phase absorption spectrum of the complex.¹⁴

The assignment proposed makes it possible to easily explain the experimentally observed simultaneous shift of Rydberg levels of series 1 ($n > 6$) and series 3 ($n > 5$), since $Rnp_{x,y}$ and $Rnd_{xz,yz}$ levels are described by the same irreducible representation Π of the $C_{\infty v}$ point group. Quantum defects decrease nearly to the same extent (by 0.24 and 0.25) on going respectively

from the $3d_{z^2} \rightarrow R4p_{x,y}$ excitation to series 1 and from $3d_{z^2} \rightarrow R4d_{xz,yz}$ to series 3, which also affirms the interpretation proposed.

The position of a peak with a maximum at 42470 cm^{-1} is intermediate between those of the members of series 1 ($n = 8$) and 3 ($n = 7$). High relative intensity of this peak (see Table 4) indicates that it is due to an individual symmetry-allowed Rydberg transition. Therefore, it can be considered as a member of one more Rydberg series (series 4). The $R8s$ state lies between the $R7d_{xz,yz}$ and $R8p_{x,y}$ levels. Hence, the peak at 42470 cm^{-1} can be assigned to the $3d_{z^2} \rightarrow R8s$ transition. In fact, the frequency calculated for this transition (42490 cm^{-1}) virtually coincides with the experimental value. The preceding member of the Rns series should lie between the $R6d_{xz,yz}$ and $R7p_{x,y}$ peaks. The only peak in this spectral region has a maximum at 41540 cm^{-1} . It is slightly (by 160 cm^{-1}) shifted toward the short-wavelength region from the calculated position, which is due to CI.

The Gaussian line with a maximum at 41080 cm^{-1} lies between members of series 2 and 3. This makes it possible to assign this line to $R6d_{z^2}$ or $R5f$ transitions that are mixed with lower-lying electronic excitations. The fact that CI occurs in this case is in agreement with the relatively large halfwidth of this spectral component (see Table 4). Increase in the principal quantum number leads to disappearance of the peaks corresponding to these transitions because of the overlap with the bands corresponding to the members of series 3.

Series 2 is mainly due to the Rydberg f excitations (their description requires decreasing the quantum defect values and the principal quantum numbers listed in Tables 1 and 3 by unity) and/or to unperturbed Rnd_{z^2} transitions. The δ value for the first member of the f series must be somewhat larger than for subsequent members of the series due to the greater penetration of the lowest Rydberg orbital.^{16,17} Therefore, its frequency will be lower than the calculated one (38190 cm^{-1}). Taking into account changes in the δ value on going from $R4s$ and $R4p_{x,y}$ to $R5s$ and $R5p_{x,y}$ excitations (see Table 2), a weak band at 37960 cm^{-1} may be assigned to the $R4f$ transition. In addition to f and d_{z^2} excitations, the Rydberg p_z transitions mixed with lower-lying valence-shell excitations might also contribute to series 2 in the spectral region above 42000 cm^{-1} . This is indicated by close energies of the $R6p_z$ transition and the member of series 2 (see Table 4).

The major problems in interpreting the spectrum of complex **1** are associated with the shifts and broadening of the Rydberg bands in the region $39000\text{--}42000\text{ cm}^{-1}$ due to CI. It is of interest to analyze the general pattern of such interactions. Particularly "sensitive" to the shifts due to mixing of electronic-excited states is the dependence of the quantum defect values of the Rydberg transitions on the principal quantum number. A diagram of the $\delta(n)$ dependence for the most reliably identified Rydberg transitions in the EAS of complex **1** is shown in Fig. 4.

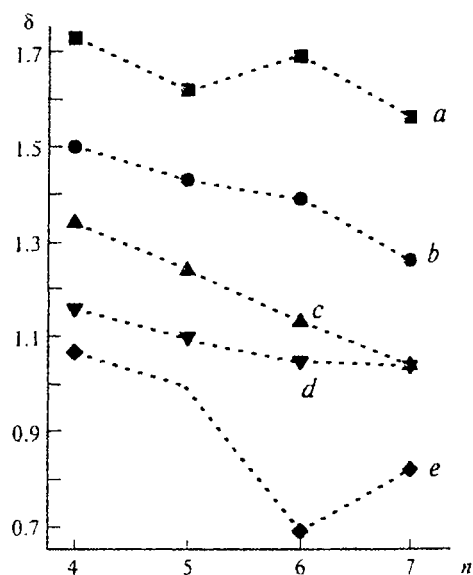


Fig. 4. Dependence of quantum defect values on the principal quantum number for transitions from the $3d_{z^2}$ orbital to Rydberg ns (a), $np_{x,y}$ (b), np_z (c), nd_{z^2} (d), and $nd_{x^2-y^2}$ levels (e) for molecule 1. For the $R5d_{xz,yz}$ transition, the δ value was assumed to be equal to the calculated value of 1.00 (see Table 3).

For all types of excitations, the first transition is characterized by an overestimated δ value (as compared to those of other transitions), which is due to the greater penetration of the lowest Rydberg MOs into the cationic core.^{16,18} For higher Rydberg levels in the absence of CI one should expect the retention of a nearly constant value of the quantum defect for the whole series, as was observed for bisarene complexes.^{4,7-13} However, in the case of compound 1 at $n > 5$ the δ values for most transitions continue to change as the principal quantum number increases (see Fig. 4).

At least two electronic-excited states (or two groups of states) perturbing the Rydberg levels can be distinguished. The first state interacts with the $R6s$, $R6p_z$, and $R7s$ levels of Σ^+ symmetry causing a blue shift and broadening of the bands corresponding to the relevant Rydberg transitions. Broadening of the bands corresponding to the Rydberg transitions from the $3d_{z^2}$ orbital can occur as a result of interaction with valence-shell excitations or with the electron transitions from the $3d_{xy,x^2-y^2}$ orbital to the Rydberg levels. However, the latter are so broad that no clearly seen corresponding bands in the EAS of complex 1 and in the spectra of other sandwich systems studied¹⁻²² can be distinguished.

The energies of Rydberg excitations from the $3d_{xy,x^2-y^2}$ MO can be estimated using typical term values for transitions from the $3d_{z^2}$ MO and the energy of electron detachment from the $3d_{xy,x^2-y^2}$ orbital, which is known from the photoelectron spectrum of complex 1.^{24,25} Such an estimate shows that the lowest Σ^+ state formed as a result of the Rydberg excitation of the

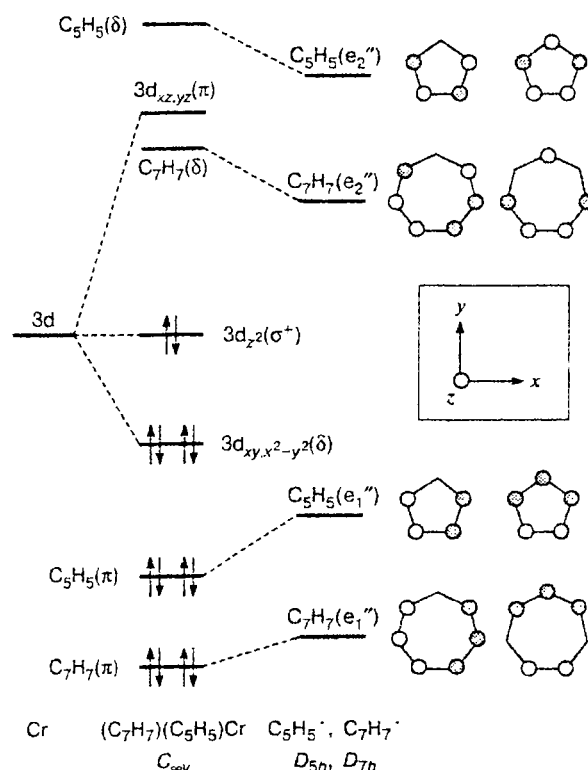


Fig. 5. Qualitative scheme of the frontier MOs in molecule 1 (see Refs. 20, 24). Shading indicates different phases of the 2p wave functions of carbon atoms of the ligand.

$3d_{xy,x^2-y^2}$ electron is in the region 45000 cm^{-1} . This excitation cannot be responsible for the blue shift of $3d_{z^2} \rightarrow R6s$ ($R6p_z$, $R7s$) transitions that have lower energies.

Among valence-shell transitions with participation of the highest occupied and lowest vacant MOs of complex 1 (Fig. 5), Σ^+ excited states are responsible for the $C_7H_7(\pi)$, $Cp(\pi) \rightarrow 3d(\pi)$ and $3d(\delta) \rightarrow C_7H_7(\delta)$, $Cp(\delta)$ transitions. Most likely, one or several Σ^+ states formed as a result of these transitions lie in the region $39000\text{--}41000\text{ cm}^{-1}$ and interact with the Rydberg levels in question.

The second group comprises the Π excited states lying between the $R6p_{x,y}$ and $R6d_{xz,yz}$ levels and being responsible for the broadening and shift of the bands corresponding to the $R6d_{xz,yz}$ and $R7p_{x,y}$ transitions and for a decrease in quantum defects of higher members of the $Rnd_{xz,yz}$ and $Rnp_{x,y}$ series. They can appear as a result of $\pi \leftrightarrow \delta$ and $\sigma^+ \leftrightarrow \pi$ excitations. Frequencies of these transitions must be of the order of 41000 cm^{-1} . Such frequencies are too high to correspond to the $3d \rightarrow 3d$ excitations in sandwich complexes of the first-row transition metals.^{29,30} On the contrary, the $C_7H_7(\pi)$, $Cp(\pi) \rightarrow Cp(\delta)$ excitations should have much higher energies, since

even in the free Cp' radical the separation between the frontier π and δ MOs exceeds 48000 cm^{-1} .³¹ Therefore, among all valence-shell transitions in molecule **1**, only $\text{C}_7\text{H}_7(\pi) \rightarrow \text{C}_7\text{H}_7(\delta)$ and $\text{Cp}(\pi) \rightarrow \text{C}_7\text{H}_7(\delta)$ transitions can effectively interact with $R6d_{xz,yz}$ and $R7p_{x,y}$ excitations.

The Π state interacting with the $R6d_{xz,yz}$ and $R7p_{x,y}$ levels may also have a Rydberg nature. The expected frequency for the $3d_{xy,x^2-y^2} \rightarrow R4p_{x,y}$ transition is $\sim 40600\text{ cm}^{-1}$. One of resulting states has Π symmetry and can be admixed to the levels corresponding to the $3d_{z^2} \rightarrow R6d_{xz,yz}$ and $3d_{z^2} \rightarrow R7p_{x,y}$ transitions. Perturbation is transmitted through the $R6d_{xz,yz}$ and $R7p_{x,y}$ states "along the chain" to higher levels belonging to these types, which results in a decrease in quantum defects for series 1 and 3 at $n > 7$ compared to the values expected for the unperturbed $Rnp_{x,y}$ and $Rnd_{xz,yz}$ excitations (see Table 3). Thus, consideration of the character of the $\delta(n)$ dependence (see Fig. 4) makes it possible not only to determine which Rydberg levels become shifted, but also specify electronic-excited states that can be responsible for these effects.

By and large, despite the problems associated with shifts of Rydberg transitions caused by Cl, our analysis made it possible to reliably interpret most of the Rydberg bands in the EAS of complex **1**. Long-wavelength peaks are due to $3d_{z^2} \rightarrow R4s$ ($R4p_{x,y}$, $R4p_z$, $R4d_{xz,yz}$) transitions. Most of the components of their vibronic structure is associated with totally symmetric metal—ring and C—H vibrations.

Series 1 and 3 correspond to excitations of the $3d_{z^2}$ electron to $Rnp_{x,y}$ and $Rnd_{xz,yz}$ levels, respectively. The decreased values of quantum defects at $n > 6$ are due to mixing of Rydberg transitions with one or several lower-lying $3d_{xy,x^2-y^2} \rightarrow R4p_{x,y}$, $\text{C}_7\text{H}_7(\pi) \rightarrow \text{C}_7\text{H}_7(\delta)$, and $\text{Cp}(\pi) \rightarrow \text{C}_7\text{H}_7(\delta)$ excitations. Transitions to Rydberg p_z , d_{z^2} , and f MOs can contribute to series 2. Shifts and broadening of bands corresponding to the Rydberg Σ^+ levels at $n = 6, 7$ are due to the admixture of valence-shell excited states corresponding to charge-transfer transitions. In the framework of the assignment made all peculiarities of the dependence of Rydberg parameters on the principal quantum number find logical explanation. The interpretation proposed is in complete agreement with the Rydberg structure in the vapor-phase spectra of cycloheptatrienyl-cyclopentadienyl complexes of molybdenum and tungsten.^{15,16}

This work was financially supported by the Russian Foundation for Basic Research (Project Nos. 96-15-97455 and 98-03-33009).

References

1. S. Yu. Ketkov, G. A. Domrachev, and G. A. Razuvaev, *Dokl. Akad. Nauk SSSR*, 1987, **292**, 890 [*Dokl. Chem.*, 1987 (Engl. Transl.)].
2. S. Yu. Ketkov, G. A. Domrachev, and G. A. Razuvaev, *Zh. Obshch. Khim.*, 1987, **57**, 967 [*J. Gen. Chem. USSR*, 1987, **57** (Engl. Transl.)].
3. S. Yu. Ketkov, G. A. Domrachev, and G. A. Razuvaev, *Opt. Spektrosk.*, 1987, **62**, 227 [*Opt. Spectrosc. USSR*, 1987, **62** (Engl. Transl.)].
4. S. Yu. Ketkov, G. A. Domrachev, and G. A. Razuvaev, *Opt. Spektrosk.*, 1987, **63**, 284 [*Opt. Spectrosc. USSR*, 1987, **63** (Engl. Transl.)].
5. S. Yu. Ketkov, G. A. Domrachev, and G. A. Razuvaev, *Zh. Fiz. Khim.*, 1987, **61**, 1682 [*J. Phys. Chem. USSR*, 1987, **61** (Engl. Transl.)].
6. G. A. Domrachev, S. Yu. Ketkov, and G. A. Razuvaev, *J. Organomet. Chem.*, 1987, **328**, 341.
7. S. Yu. Ketkov, G. A. Domrachev, and G. A. Razuvaev, *Metalloorg. Khim.*, 1988, **1**, 40 [*Organomet. Chem. USSR*, 1988, **1** (Engl. Transl.)].
8. S. Yu. Ketkov, G. A. Domrachev, and G. A. Razuvaev, *J. Mol. Struct.*, 1989, **195**, 175.
9. S. Yu. Ketkov and G. A. Domrachev, *J. Organomet. Chem.*, 1990, **389**, 187.
10. A. Penner, A. Amirav, S. Tasaki, and R. Bersohn, *J. Chem. Phys.*, 1993, **99**, 176.
11. S. Yu. Ketkov, J. C. Green, and C. P. Mehnert, *J. Chem. Soc., Faraday Trans.*, 1997, **93**, 2461.
12. S. Yu. Ketkov, G. A. Domrachev, C. P. Mehnert, and J. C. Green, *Izv. Akad. Nauk. Ser. Khim.*, 1998, 897 [*Russ. Chem. Bull.*, 1998, **47**, 868 (Engl. Transl.)].
13. S. Yu. Ketkov, C. P. Mehnert, and J. C. Green, *Chem. Phys.*, 1996, **203**, 245.
14. S. Yu. Ketkov, *J. Organomet. Chem.*, 1992, **429**, C38.
15. S. Yu. Ketkov and J. C. Green, *J. Chem. Soc., Faraday Trans.*, 1997, **93**, 2467.
16. J. C. Green, M. L. H. Green, C. N. Field, D. K. P. Ng, and S. Yu. Ketkov, *J. Organomet. Chem.*, 1995, **501**, 107.
17. S. Yu. Ketkov, *Opt. Spektrosk.*, 1992, **72**, 1088 [*Opt. Spectrosc.*, 1992, **72** (Engl. Transl.)].
18. S. Yu. Ketkov, *J. Organomet. Chem.*, 1994, **465**, 225.
19. S. Yu. Ketkov, *Izv. Akad. Nauk. Ser. Khim.*, 1994, 634 [*Russ. Chem. Bull.*, 1994, **43**, 583 (Engl. Transl.)].
20. J. C. Green and S. Yu. Ketkov, *Organometallics*, 1996, **15**, 4747.
21. S. Yu. Ketkov and G. A. Domrachev, *Inorg. Chim. Acta*, 1990, **178**, 233.
22. S. Yu. Ketkov and G. A. Domrachev, *J. Organomet. Chem.*, 1991, **420**, 67.
23. H. O. van Oven, C. J. Groenenboom, and H. J. de Liefde Meijer, *J. Organomet. Chem.*, 1974, **81**, 379.
24. S. Evans, J. C. Green, S. E. Jackson, and B. Higginson, *J. Chem. Soc., Dalton Trans.*, 1974, 304.
25. C. E. Davies, I. M. Gardiner, J. C. Green, N. J. Hazel, P. D. Grebenik, V. S. Mtetwa, and K. Prout, *J. Chem. Soc., Dalton Trans.*, 1985, 669.
26. H. W. Werner, E. O. Fischer, and J. Müller, *Chem. Ber.*, 1970, **103**, 2258.
27. S. J. Cyvin, J. Brunvoll, and L. Schäfer, *J. Chem. Phys.*, 1971, **54**, 1517.
28. M. B. Robin, *Higher Excited States of Polyatomic Molecules*, Academic Press, New York, 1985, **3**.
29. K. D. Warren, *Struct. Bonding (Berlin)*, 1976, **27**, 45.
30. S. Y. Sohn, D. N. Hendrickson, and H. B. Gray, *J. Am. Chem. Soc.*, 1971, **93**, 3603.
31. E. S. J. Robles, A. M. Ellis, and T. A. Miller, *J. Phys. Chem.*, 1992, **96**, 8791.

Received March 5, 1999